

MOLECULAR GAS AROUND THE DOUBLE NUCLEUS IN M83

KAZUSHI SAKAMOTO,¹ SATOKI MATSUSHITA,² ALISON B. PECK,¹ MARTINA C. WIEDNER,^{1,3} AND DAISUKE IONO^{1,4}

Received 2004 January 26; accepted 2004 March 4; published 2004 October 28

ABSTRACT

The center of M83, a barred starburst galaxy with a double nucleus, has been observed in the CO ($J = 2-1$) and CO ($J = 3-2$) lines with the Submillimeter Array. The molecular gas shows a distribution and kinematics typical for barred galaxies at ~ 1 kpc radii but reveals unusual kinematics around the double nucleus in the central ~ 300 pc. Our CO velocity data show that the visible nucleus in M83 is at least $3''$ (65 pc) away from the galaxy's dynamical center, which most likely coincides with the center of symmetry previously determined in the K band and is suggested to host another nucleus. We discovered high-velocity molecular gas associated with the visible off-center nucleus and also found a steep velocity gradient across it. We attribute these features to a gas disk rotating around the off-center nucleus, which may be the remnant of a small galaxy accreted by M83. The dynamical mass of this component is estimated to be $3 \times 10^8 M_{\odot}$ within a radius of 40 pc. The dynamical perturbation from the off-center nucleus may have played a key role in shaping the lopsided starburst.

Subject headings: galaxies: individual (M83, NGC 5236) — galaxies: ISM —
galaxies: kinematics and dynamics — galaxies: nuclei — galaxies: starburst

1. INTRODUCTION

M83 (NGC 5236) is a nearby face-on barred spiral galaxy with a double nucleus and a nuclear starburst ($D = 4.5$ Mpc, $1'' = 22$ pc; Thim et al. 2003). The galaxy is exceptionally complex in the central 300 pc, despite the symmetric appearance of its bar and spiral arms. In the K band, the brightest point, called the “visible nucleus,” is offset by $3.4''$ (75 pc) from the centroid (i.e., center of symmetry) determined from the isophotes at radii of 0.3–0.7 kpc (Thatte et al. 2000, hereafter T00). The centroid suffers from large extinction and does not show a peak in the K band. However, the stellar velocity dispersion peaks both at the visible nucleus and near the isophotal centroid, and suggests a mass of $\sim 10^7 M_{\odot}$ for each. This suggests a double nucleus (T00). The visible nucleus has a hard power-law spectrum in X-ray that is due to either an accreting supermassive black hole or X-ray binaries (Soria & Wu 2002). Elmegreen et al. (1998) found a double circumnuclear ring in their $J-K$ color index map. The “inner” and “outer” rings of 190 and 60 pc radius, respectively, are not concentric. The galaxy hosts a circumnuclear starburst mainly in the “starburst arc” of ~ 250 pc length that lies between the two rings (Gallais et al. 1991; Harris et al. 2001). The galactic center has a large amount of molecular gas, estimated to be $10^{7.5} - 10^{8.5} M_{\odot}$ in $r \leq 300$ pc (Handa et al. 1990; Israel & Baas 2001).

The proximity, face-on configuration, abundant molecular gas, starburst, and double nucleus make M83 one of the most interesting targets to study spiral galaxies and their nuclear activity through molecular gas. We observed M83 as a part of the early science program of the Submillimeter Array (SMA).⁵ The new telescope in Hawaii can easily observe the galaxy at

$\delta = -30^\circ$. In this Letter, we first describe the observations and the bar-driven gasdynamics in the central 2 kpc, and then we show that the visible nucleus is indeed offset from the dynamical center of M83 and has a velocity feature indicative of its own gas disk. We discuss the origin of the double nucleus and its relation to the starburst activity.

2. SMA OBSERVATIONS

M83 was observed with the SMA (Ho et al. 2004) from 2003 February through May during the commissioning of the array. We observed CO ($J = 2-1$) and CO ($J = 3-2$) lines in the galactic center with a total on-source time of 14 and 10 hr, respectively. Five of the eight SMA antennas were available, except for the first 230 GHz observations, which had only four antennas. A partial reconfiguration of the array during our observing period gave us 14 independent baselines for each band. Zenith opacity was between 0.03 and 0.15 at 225 GHz during our observations, and double sideband system temperatures toward the galaxy were typically 150 K at 1.3 mm and 500 K at 0.85 mm. The correlator bandwidth and resolution were 640 and 0.8125 MHz, respectively. The CO (2–1) observations were the first mosaic imaging with the SMA. Three positions separated by $25''$ from each other along the bar were cycled through every 10 minutes. We calibrated the system gain every ~ 30 minutes by observing a pair of nearby quasars, J1337–129 and J1316–336 at 1.3 mm and J1337–129 and 3C 279 at 0.85 mm. Interferometric pointing was made during the observations toward the gain calibrators to keep pointing errors $\lesssim 5''$. The passband was calibrated using Jupiter or Saturn, and the flux scale using Uranus. The primary calibrator J1337–129 dimmed by $\sim 30\%$ in 1.3 mm in our observing period of 76 days.

Calibration of the raw data was made using the MIR package, and the imaging and data analysis were made with MIRIAD and AIPS. Channel maps were made every 10 km s^{-1} and then combined to make moment maps. No continuum was detected from channels free of line emission, with 5σ upper limits of 50 and $150 \text{ mJy beam}^{-1}$ for 1.3 and 0.85 mm, respectively. Our interferometric maps recovered 90% and 30%–50% of the total flux at the galactic center in CO (2–1) and CO (3–2), respectively, based on a comparison with single-dish obser-

¹ Harvard-Smithsonian Center for Astrophysics, Submillimeter Array, 645, North A'ohoku Place, Hilo, HI 96720.

² Academia Sinica Institute of Astronomy and Astrophysics, P.O. Box 23-104, Taipei 106, Taiwan.

³ Physikalisches Institut, Universität zu Köln, Zùlpicher Strasse 77, 50937 Köln, Germany.

⁴ Department of Astronomy, University of Massachusetts at Amherst, LGRT-B619E, 710 North Pleasant Street, Amherst, MA 01002.

⁵ The Submillimeter Array is a joint project between the Smithsonian Astrophysical Observatory and the Academia Sinica Institute of Astronomy and Astrophysics, and is funded by the Smithsonian Institution and the Academia Sinica.

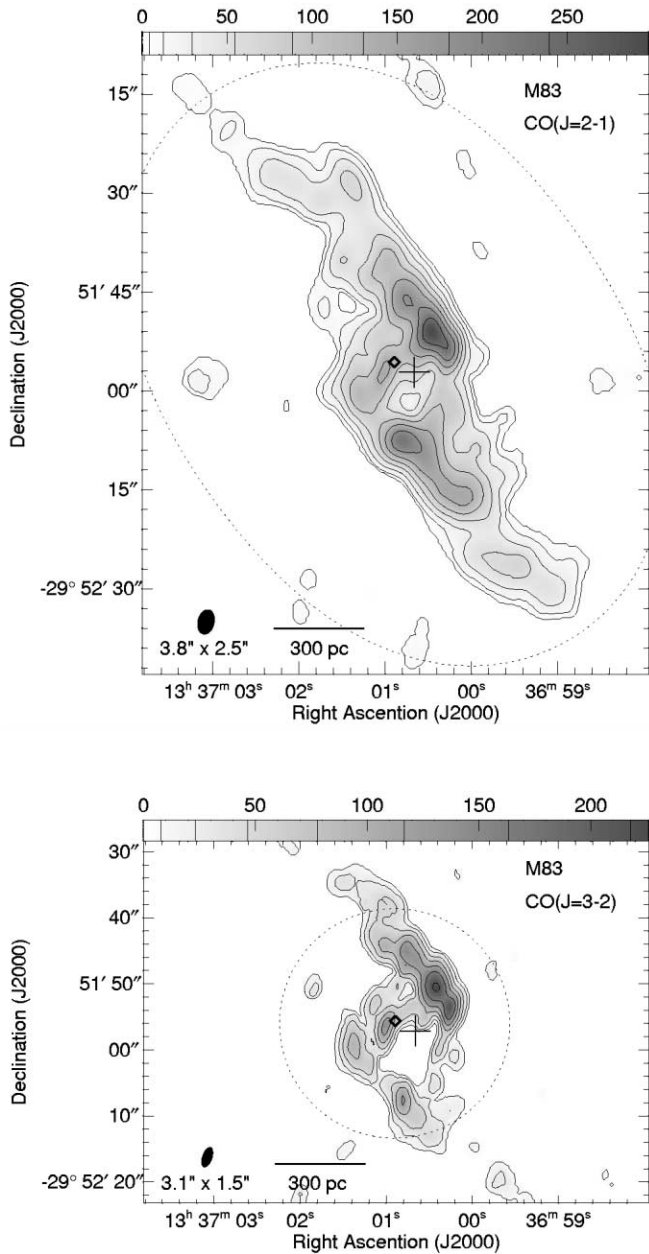


FIG. 1.—Integrated intensity maps of CO (2–1) and CO (3–2) in the center of M83. The diamond marks the visible nucleus, and the plus sign is at the isophotal centroid in the K band. The synthesized beam of each map is shown at the bottom left-hand corner. The unit of intensity is $\text{Jy beam}^{-1} \text{ km s}^{-1}$. The dotted contour in the CO (2–1) map shows where the power pattern of the mosaicked primary beam drops to 30% of its peak. The one in the CO (3–2) map shows the half-power width of the primary beam. The maps are not corrected for the power (i.e., sensitivity) patterns.

vations (Crosthwaite et al. 2002; Dumke et al. 2001; Israel & Baas 2001).

3. MOLECULAR GAS IN THE CENTRAL 2 KILOPARSECS

The CO (2–1) and CO (3–2) integrated intensity maps (Fig. 1) reveal two gas ridges at the leading side of the stellar bar (with a position angle [P.A.] of $\sim 50^\circ$) and a nuclear gas ring of ~ 300 pc diameter. There are additional features inside the ring, which we discuss in § 4. The overall morphology of molecular gas agrees well with that in the J – K image, which

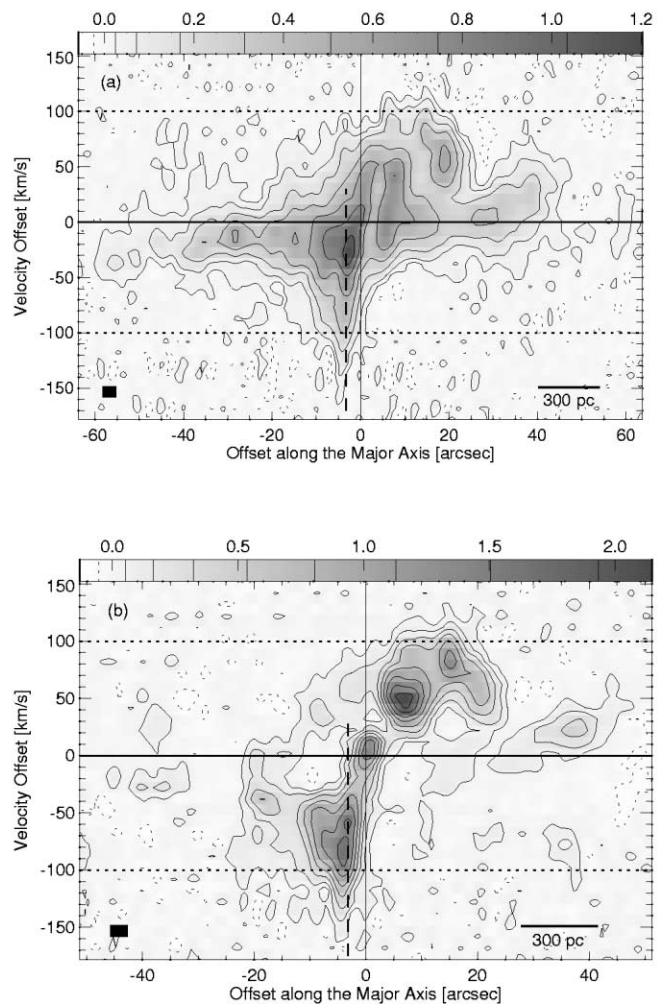


FIG. 2.—CO (2–1) position-velocity diagrams along the major axis (P.A. = 226°). Position is measured from the isophotal centroid, and velocity is from the systemic velocity of 508 km s^{-1} . The intensity unit is Jy beam^{-1} . The black rectangles in the bottom left-hand corners show spatial and velocity resolutions. The dashed lines at $-3''$ and $2''$ mark the position of the visible nucleus. (a) The cut (or “slit”) is $30''$ wide and includes most emission in our mosaic. (b) The cut is $5''$ wide, with its central axis $1''$ offset from the major axis so that it crosses the visible nucleus. Most of the linear gas ridges lie outside this cut.

approximately traces extinction, of Elmegreen et al. (1998); for example, the ~ 300 pc nuclear ring is their outer ring.

The pair of ridges and the nuclear ring must be due to the two types of oval orbits in the bar. Namely, the former must be on the x_1 orbits, which are the dominant type of orbits in a bar and are elongated along the bar, while the latter must be on the x_2 orbits, which are seen near the center of a bar and are elongated perpendicular to the bar (see Athanassoula 1992). The presence of two major kinematical components is evident in the position-velocity diagram of the CO (2–1) emission (Fig. 2a). One component that runs throughout our field of view with slow rotation is from the gas ridges, while the other with faster rotation near the center is from around the nuclear ring ($r \approx 8''$). Our viewing angle of M83, from which the line of nodes coincides with the bar, makes gas on x_1 orbits appear slower and x_2 gas appear faster.

Besides the ridges and the nuclear ring, there is faint emission between them in the CO (2–1) map (Fig. 1, top). This weak emission and part of the gas ridges form a parallelogram. The morphology and location of this component suggest that it is

on oval orbits whose major axes are neither perpendicular nor parallel to the bar but in-between. Indeed, it is theoretically expected that gaseous orbits between x_1 - and x_2 -dominated regions continuously change their major axes from parallel to the bar to perpendicular to the bar as the orbital radius decreases (Wada 1994; Lindblad & Lindblad 1994). In addition, gas funneled in the bar through one of the gas ridges on x_1 orbits can eventually collide with gas in the nuclear ring on x_2 orbits and can be “sprayed back” onto the other ridge to form a parallelogram (Binney et al. 1991; Regan et al. 1999).

4. MOLECULAR GAS IN THE CENTRAL 300 PARSECS

We established kinematically the offset of the visible nucleus from the dynamical center in the following way. The systemic velocity of the galaxy was first determined to be $508 \pm 3 \text{ km s}^{-1}$ (V_{LSR}) from the CO (2–1) mean velocity data (Fig. 3) by searching for the velocity whose contour is least biased toward either the blue- or the redshifted direction. The velocity map was not fitted to derive the systemic velocity because the emission covered only a small area and because there is non-circular motion due to the bar⁶ and to the visible nucleus as discussed below. The dynamical center should lie on the systemic-velocity contour. The K -band center determined by T00 from isophotes at radii between $12''$ and $30''$, shown as a cross in the velocity map, is almost on that contour. Thus, it is most likely that the dynamical center of M83 is on, or in the vicinity of, the isophotal centroid, as morphologically expected. On the other hand, the visible nucleus shown as a diamond in the velocity map is clearly off the systemic-velocity contour and must be at least $3''$ (65 pc) away from the dynamical center.

We discovered high-velocity gas around the off-center, visible nucleus. In Figure 2, where the off-center nucleus is at $-3''.2$ while the isophotal centroid is at $0''$, the position-velocity diagrams show a high-velocity component at around $-5''$ and -160 km s^{-1} . There is no counterpart in the receding side; the largest velocity at $+5''$ is $+120 \text{ km s}^{-1}$. Spatially, the component is compact and is within $2''$ of the off-center nucleus at the most blueshifted velocity. This compact high-velocity component is detected in both CO (2–1) and CO (3–2). It shows up in the integrated intensity maps as the peak $\sim 2''$ southeast of the visible nucleus. The large blueshift of this component is also evident in the mean velocity map (Fig. 3). The position-velocity diagram in Figure 2b clearly shows that the high-velocity gas is a part of the continuous ridge of emission that has a large velocity gradient across the visible, off-center nucleus. The velocity gradient around the nucleus is roughly along the galaxy’s major axis, as seen in the mean velocity map.

We interpret this feature as a gas disk that rotates around the off-center nucleus but not directly around the dynamical center of M83. The feature is unlikely to be due to streaming motion in the bar potential, although molecular gas in the center of barred galaxies often shows a large velocity gradient due to noncircular motion (e.g., Sakamoto et al. 2000). This is because the feature is seen only on one side of the dynamical center and only in blueshifted velocities, and also because the visible nucleus is at the center of the feature. The feature is also unlikely to be due to an outflow. This is because both starburst

⁶ We adopt the P.A. of 226° for the receding major axis of the galaxy, based on the CO and H I velocity fitting across the disk (Crosthwaite et al. 2002). In Fig. 3, the contour for the systemic velocity has an angle of $\sim 75^\circ$ rather than 90° to this major axis. Noncircular motion in the bar is probably most responsible for this, although warp of the disk could be partly responsible.

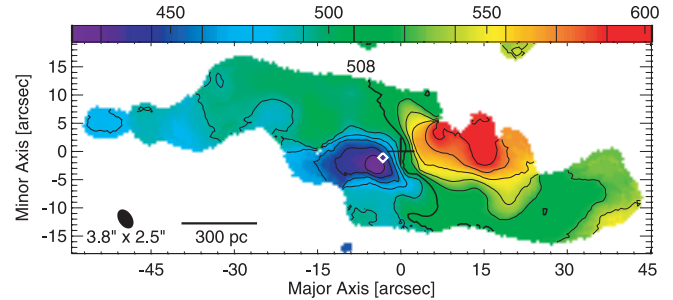


FIG. 3.—CO (2–1) velocity map of M83. Contours are in 16 km s^{-1} steps from 428 km s^{-1} (V_{LSR}). The systemic velocity of 508 km s^{-1} is shown by a thick contour. The diamond at $(-3''.2, -1''.1)$ is the visible nucleus, and the plus sign at $(0, 0)$ is the K -band isophotal centroid. The map is rotated to make the major axis horizontal.

and a nuclear jet, the latter of which may exist along the minor axis of the galaxy (Cowan et al. 1994), would cause a velocity gradient along the minor axis rather than the major axis as we see here.

The extent and the total width of the line-of-sight velocity of this component are 80 pc and 140 km s^{-1} , respectively, or 120 pc and 180 km s^{-1} if we include the peak near $(+1'', +10 \text{ km s}^{-1})$. The size and location of the gas disk are roughly consistent with those of the inner ring in Elmegreen et al. (1998). The dynamical mass of the disk is $3 \times 10^8 M_\odot$ within a radius of 40 pc assuming the same inclination as M83 (25°); it would be a factor of 4 smaller if the inclination was 60° . The mass distribution in the disk is extended, and not dominated by a single compact object, because the mass within 6.5 pc of the visible nucleus was estimated to be $1.6 \times 10^7 M_\odot$ (T00).

What are the off-center nucleus and the gas rotating around it? T00 concluded that the visible nucleus could not be a young star cluster, but had to be a dynamically hot nucleus, on the basis of its high-velocity dispersion and stellar population. This conclusion is consistent with the observation of Harris et al. (2001) that the mass of the individual young clusters in the nuclear region of M83 (mostly on the starburst arc) is less than about $10^5 M_\odot$. The eccentric disk model used for the double nucleus in M31 (Tremaine 1995) is also dismissed for M83 because, among other things, the rotation of stars and gas around the dynamical center is not Keplerian.

A plausible model for the visible off-center nucleus is that it is the remnant core of a small galaxy that merged into M83. The prototype major merger Arp 220 has two surviving nuclei at a projected separation of $\sim 300 \text{ pc}$ with gas disks rotating around each of them (Sakamoto et al. 1999; Genzel et al. 2001). A less violent minor merger may have produced the configuration seen here. M83 has a faint stellar arc of $\sim 30 \text{ kpc}$ length indicating the accretion of at least one satellite (Malin & Hadley 1997). If the visible nucleus came from outside, then it does not need to be on the disk plane of M83. However, the nucleus is probably not far away from the midplane of M83 because (1) the chances of seeing it at the small projected distance from the dynamical center are low if the nucleus is far from the disk plane, (2) the mean velocity of gas and stars of the visible nucleus is roughly on the rotation curve of M83, and (3) numerical simulations of satellite accretion show that a satellite rapidly loses its orbital radius after it settles on the disk of the larger galaxy, since disk stars are the main source of torque on the satellite (Walker et al. 1996). If the accreted nucleus has spent a long time in the galactic plane of M83, then the gas

rotating around the nucleus, presumably as a minidisk, may not be from the original satellite but may have been captured from M83 during the accretion. Regarding the large extinction toward the other nucleus at the dynamical center (presumably the true nucleus of M83), it is conceivable that the minidisk is slightly above the midplane of M83 in the direction of the hidden nucleus, effectively shielding most of the light from it even though the CO-integrated intensities are not particularly high toward the dynamical center.

Alternatively, the visible nucleus may be a part of the original nucleus of M83 that has moved away from the dynamical center of the galaxy. This would explain the lack of obvious disturbance in the M83 disk outside the nuclear ring. Such a wandering nucleus may occur even without perturbation from outside the galaxy (Taga & Iye 1998 and references therein).

5. NUCLEAR STARBURST

The starburst in M83 is lopsided, mostly on the receding side of the dynamical center. This is true not only for the starburst arc (Fig. 4) but also for other sites of active star formation more obscured by dust. The latter are $\sim 10''$ northwest of the visible nucleus, near the strongest peak of CO emission, according to radio and mid-infrared observations (Turner & Ho 1994; Telesco et al. 1993; Rouan et al. 1996).

The lopsided starburst may well be due to the dynamical effect of the off-center nucleus. Lopsidedness ($m = 1$ mode) is atypical in starburst morphology near the center of a barred galaxy, where bisymmetry (i.e., $m = 2$ mode such as twin peaks, a two-armed spiral, and an oval ring) is most often observed. Our observations established that the visible nucleus, be it an intruder or a wanderer, is off the dynamical center of the galaxy. The new mass estimate of this component is $\sim 20\%$ of the dynamical mass in the central 300 pc of M83. Thus, the off-center nucleus must have had a significant, both positive and negative, influence on star formation in the area through perturbations to star-forming gas. It is noteworthy that both the age of the starburst and the dynamical timescale for the off-center nucleus are on the order of several megayears. To summarize, the nuclear starburst of M83 owes much to the bar-driven gasdynamics for accumulating molecular gas toward the

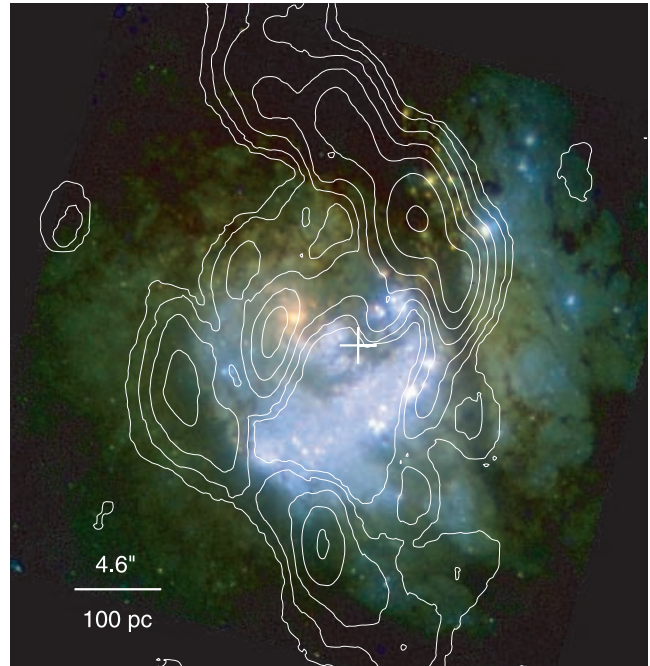


FIG. 4.—Center of M83. SMA CO (3–2) contours (same as in Fig. 1) are overlaid on a three-color composite made from archival *HST*/WFPC2 data. F300W, F547M, and F814W images are used for blue, green, and red, respectively. The visible nucleus is the orange peak, while the *K*-band centroid, which probably coincides with the dynamical center, is marked with the plus sign. The starburst arc is in white-blue and has little CO (3–2) emission on it.

central 300 pc, and it appears to have taken the current shape under the strong influence of the double nucleus.

We are grateful to all the people who worked hard to realize the SMA. We also thank P. T. P. Ho and J. M. Moran for helpful comments on the manuscript, N. Z. Scoville for providing us with the MIR package before its release, and STScI for the archival *HST* images of M83.

REFERENCES

- Athanassoula, E. 1992, *MNRAS*, 259, 345
 Binney, J., Gerhard, O. E., Stark, A. A., Bally, J., & Uchida, K. I. 1991, *MNRAS*, 252, 210
 Cowan, J. J., Roberts, D. A., & Branch, D. 1994, *ApJ*, 434, 128
 Crosthwaite, L. P., Turner, J. L., Buchholz, L., Ho, P. T. P., & Martin, R. N. 2002, *AJ*, 123, 1892
 Dumke, M., Nieten, Ch., Thuma, G., Wielebinski, R., & Walsh, W. 2001, *A&A*, 373, 853
 Elmegreen, D. M., Chromey, F. R., & Warren, A. R. 1998, *AJ*, 116, 2834
 Gallais, P., Rouan, D., Lacombe, F., Tiphène, D., & Vauglin, I. 1991, *A&A*, 243, 309
 Genzel, R., Tacconi, L. J., Rigopoulou, D., Lutz, D., & Tecza, M. 2001, *ApJ*, 563, 527
 Handa, T., Nakai, N., Sofue, Y., Hayashi, M., & Fujimoto, M. 1990, *PASJ*, 42, 1
 Harris, J., Calzetti, D., Gallagher, J. S., III, Conselice, C. J., & Smith, D. A. 2001, *AJ*, 122, 3046
 Ho, P. T. P., Moran, J. M., & Lo, K. Y. 2004, *ApJ*, 616, L1
 Israel, F. P., & Baas, F. 2001, *A&A*, 371, 433
 Lindblad, P. O., & Lindblad, P. A. B. 1994, in *ASP Conf. Ser. 66, Physics of the Gaseous and Stellar Disks of the Galaxy*, ed. A. M. Fridman (San Francisco: ASP), 29
 Malin, D., & Hadley, B. 1997, *Publ. Astron. Soc. Australia*, 14, 52
 Regan, M. W., Sheth, K., & Vogel, S. N. 1999, *ApJ*, 526, 97
 Rouan, D., et al. 1996, *A&A*, 315, L141
 Sakamoto, K., Baker, A. J., & Scoville, N. Z. 2000, *ApJ*, 533, 149
 Sakamoto, K., Scoville, N. Z., Yun, M. S., Crosas, M., Genzel, R., & Tacconi, L. J. 1999, *ApJ*, 514, 68
 Soria, R., & Wu, K. 2002, *A&A*, 384, 99
 Taga, M., & Iye, M. 1998, *MNRAS*, 299, 111
 Telesco, C. M., Dressel, L. L., & Wolstencroft, R. D. 1993, *ApJ*, 414, 120
 Thatte, N., Tecza, M., & Genzel, R. 2000, *A&A*, 364, L47 (T00)
 Thim, F., Tammann, G. A., Saha, A., Dolphin, A., Sandage, A., Tolstoy, E., & Lbhardt, L. 2003, *ApJ*, 590, 256
 Tremaine, S. 1995, *AJ*, 110, 628
 Turner, J. L., & Ho, P. T. P. 1994, *ApJ*, 421, 122
 Wada, K. 1994, *PASJ*, 46, 165
 Walker, I. R., Mihos, C. J., & Hernquist, L. 1996, *ApJ*, 460, 121